JOC The Journal of Organic Chemistry

Article

pubs.acs.org/joc

$^1J_{CH}$ NMR Profile: Identification of Key Structural Features and Functionalities by Visual Observation and Direct Measurement of One-Bond Proton-Carbon Coupling Constants

Núria Marcó,[†] Alexandre A. Souza,[†,∥] Pau Nolis,[†] Carlos Cobas,[‡] Roberto R. Gil,[§] and Teodor Parella*[,†]

[†]Servei de Ressonància Magnètica Nuclear, Universitat Autònoma de Barcelona, E-08193 Bellaterra (Barcelona) Catalonia, Spain

[‡]Mestrelab Research, Santiago de Compostela, E-15706 A Coruña, Spain

[§]Department of Chemistry, Carnegie Mellon University, Pittsburgh, Pennsylvania 15213, United States

[∥]Departamento de Química, Universidade Federal do Piauí, Teresina, PI 64049-550, Brazil

Supporting Information

ABSTRACT: A user-friendly NMR interface for the visual and accurate determination of experimental one-bond proton-carbon coupling constants ($^1J_{CH}$) in small molecules is presented. This intuitive $^1J_{CH}$ profile correlates directly to $\delta(^1H)$, and $^1J_{CH}$ facilitates the rapid identification and assignment of ^1H signals belonging to key structural elements and functional groups. Illustrative examples are provided for some target molecules, including terminal alkynes, strained rings, electronegative substituents, or lone-pair-bearing heteronuclei.

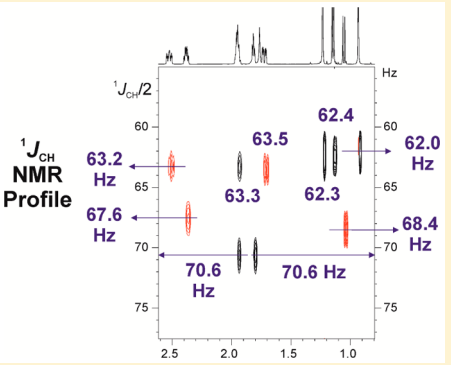

INTRODUCTION

Heteronuclear one-bond proton-carbon coupling constants ($^1J_{CH}$) offer a wealth of structural, stereochemical, and conformational information in small synthetic and natural products in solution.[1] As a general trend, $^1J_{CH}$ values range from 120 to 250 Hz, typically 120−140 Hz for aliphatic, 140−170 Hz for olefinic or aromatic, 170−200 Hz in characteristic aromatic heterocycles, and around 250 Hz in terminal alkynes. The magnitude of $^1J_{CH}$ is directly related to the *s* character of the CH bond and also is strongly influenced by the nature of substituents on the carbon center and on its surroundings. Within the last four decades, a large number of scientific publications demonstrating the success of these couplings to identify key structural features and functional groups have been extensively reported. For instance, characteristic $^1J_{CH}$ couplings are fundamental to determine the anomeric α/β configuration in hexopyranoses, to assign sp triple bond protons, to characterize aromatic heterocycles, and to confirm the presence of electronegative nuclei (oxygen, chlorine or bromine, etc.) or of strained ring systems such as cyclopropanes, epoxides, cyclobutanes, or fused bicycle systems (norbornanes, pinanes, etc.).[1]

$^1J_{CH}$ values are currently determined from well-defined doublets along the direct F_2[2,3] or the indirect F_1[4] dimensions in modern HSQC experiments. These measurements are usually performed by determining the distance in hertz between the two separated components of each individual cross-peak, although more sophisiticated approaches involving simulations and *J* modulations have also been proposed.[5] In general, most of these studies have concentrated on the accuracy, general applicability, and the simplicity of such measurements. We propose here a completely new and complementary approach to visualize, analyze, and even determine directly and precisely $^1J_{CH}$ values in a very straightforward way. Our method is based on the generation of a helpful $^1J_{CH}$ NMR profile that allows the observation of the complete range of $^1J_{CH}$ existing in a given molecule at a glance. This 2D $^1J_{CH}$ profile correlates directly $\delta(^1H)$ and $^1J_{CH}$, and it can be interpreted like an NMR chromatography, where ^1H signals at the detected F_2 dimension are dispersed by their $^1J_{CH}$ in F_1, resembling the popular DOSY representation, where ^1H signals are dispersed as a function of their diffusion coefficients.[6]

RESULTS AND DISCUSSION

For this purpose, we have designed a novel *J*-resolved HSQC (HSQC-$^1J_{CH}$) pulse scheme that contains three sequential steps (Figure 1): (i) an initial 1D ^{13}C isotope filter based on the multiplicity-edited (ME) HSQC pulse timing to select ^1H directly attached to ^{13}C;[7] (ii) a *J*-resolved block based on the

Received: December 1, 2016
Published: January 9, 2017

DOI: 10.1021/acs.joc.6b02873
J. Org. Chem. 2017, 82, 2040−2044

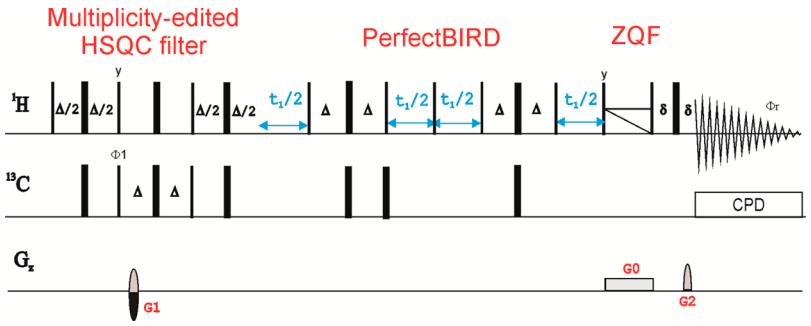

Figure 1. General pulse scheme to record two-dimensional HSQC-$^1J_{CH}$ experiments. Thin and thick rectangles represent 90 and 180° rectangular pulses, respectively, applied along the *x* axis unless indicated differently. A basic two-step phase cycling is applied: $\phi_1 = x,-x$; $\phi_{rec} = x,-x$. Inversion and refocusing 180° ^{13}C pulses can be applied as adiabatic pulses. The interpulse delays in INEPT and BIRD elements are optimized according to $\Delta = 1/(2*^1J_{CH})$. The ratio between gradients G1/G2 was 80:20.1, and the final ZQF consists of a chirped adiabatic pulse applied simultaneously to a rectangular gradient (G0). The echo/antiecho encoding in F1 was achieved by changing the sign of G1 between successive t_1 increments. More details can be found in the Supporting Information.

perfectBIRD element[3c] to allow the exclusive evolution of $^1J_{CH}$, whereas $^2J_{HH}$ values are efficiently refocused; and (iii) a final zero-quantum filter (ZQF)[8] prior to acquisition to remove any unwanted dispersive contribution to the line shapes.

This experiment initially produces a symmetrical spectrum with respect to $F_1 = 0$, where, in an unprecedented way, all ^1H signals show a clean doublet along the F_1 dimension due to $^1J_{CH}$, irrespective of their methine, methylene, or methyl nature. As a proof of concept, Figure 2A shows the superb features of the 140 Hz optimized HSQC-$^1J_{CH}$ spectrum of the alkaloid strychnine (**1**), where signals present a pure in-phase character in F_1 with respect to $^1J_{CH}$, whereas their relative positive/negative phase generated by the ME block allows a quick distinction between CH/CH_3 (up) and CH_2 (down) protons. In order to further facilitate the qualitative and quantitative analysis of this simple spectrum, the alternative visualization and analysis of only one part of the spectrum, the so-called $^1J_{CH}$ NMR profile, is proposed (Figure 2B). Taking advantage of its symmetry, we reconstructed half of the spectrum by a simple spectral self-combination postprocessing (an automated algorithm is available for Mnova software package). The $^1J_{CH}$ profile affords a very useful interface to quickly identify characteristic $^1J_{CH}$ values that can confirm the existence of particular structural features and/or functional groups in an unknown structure. Assuming that HSQC-$^1J_{CH}$ experiments will be recorded once the assignment of both ^1H and ^{13}C chemical shifts would already been established by traditional NMR methods, the interpretation of the $^1J_{CH}$ NMR profile becomes obvious, easy, and fast. Each ^1H signal appears just to the coordinate $^1J_{CH}/2$ along F_1, allowing a direct determination of $^1J_{CH}$ and an overall visualization of the full range of existing $^1J_{CH}$ values in the molecule. For instance, a complete set of experimental $^1J_{CH}$ ranging from 124.2 to 168.2 Hz is observed in **1** that can be related to several functionalities and structural features present in the molecular structure. First, the large difference of 15.7 Hz observed for the diastereotopic H18a (145.9 Hz) and H18b (130.2 Hz) protons can be attributed to the Perlin effect, which correlates $^1J_{CH}$ to the lone-pair orientation of the neighboring N19 amine nitrogen. In this case, $^1J_{CH}$ is larger when the respective CH bond is *cis* to the nitrogen lone pair than when it is in a *trans* rearrangement.[9] Similar effects are observed for the aliphatic H16 (146.4 Hz) and H8 (144.9 Hz) methine protons and for H12 (149.1 Hz), which is adjacent to an oxygen nucleus. Also the relative orientation of H11a and H11b protons with respect to the

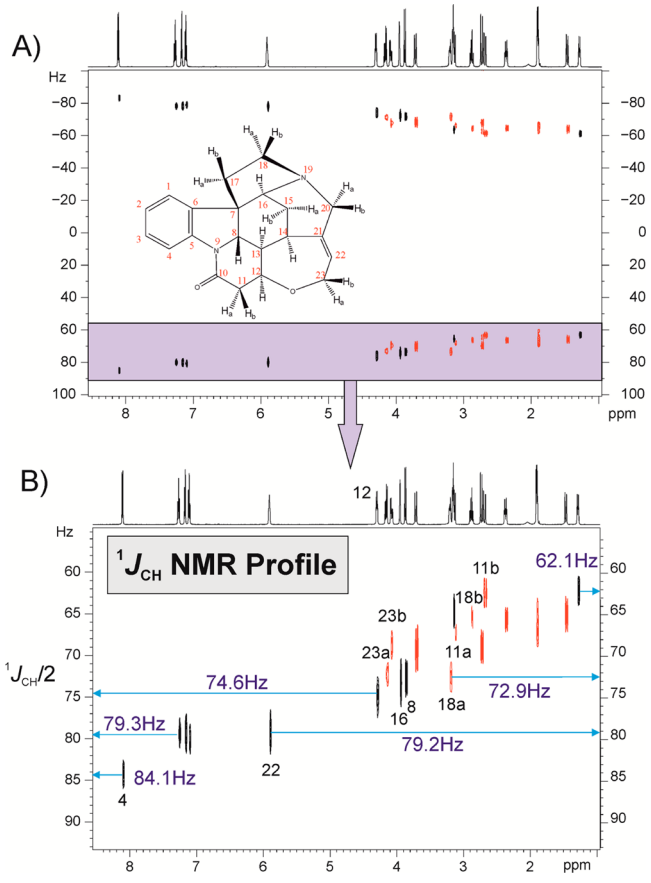

Figure 2. (A) 600.13 MHz 2D HSQC-$^1J_{CH}$ spectrum of strychnine (**1**) in $CDCl_3$ from which $^1J_{CH}$ could be extracted from the clean doublet in F_1 for each individual ^1H signal. (B) Graphical and more intuitive $^1J_{CH}$ NMR profile from which the magnitude of $^1J_{CH}/2$ (in Hz) can be directly obtained from the F_1 coordinate of each cross-peak. Illustrative $^1J_{CH}$ values are given in hertz for some selected peaks. Positive black peaks correspond to CH/CH_3, and negative red peaks are CH_2. See more detailed expanded areas in Figure S1.

carbonyl C10 can be established by the large difference of their $^1J_{CH}$ (134.2 vs 124.7, respectively) and the larger $^1J_{CH}$ of H4 (about 10 Hz) compared to that of the other aromatic protons, which is attributed to the presence of the N9 amide group in its *ortho* position. Finally, the H23a/b protons (144.4 and 136.3 Hz, respectively) are a good example showing how $^1J_{CH}$ values

DOI: 10.1021/acs.joc.6b02873
J. Org. Chem. 2017, 82, 2040−2044

smaller than expected are the result of the opposite effect between Perlin and hyperconjugative (C−H) → π* interactions.[1b]

The $^1J_{CH}$ data extracted from the profile manually or from an automated peak picking correlate very well with those determined by measuring individually each doublet along F_1 from the spectrum of Figure 2A and also agree with experimental data measured from other NMR methods in previous works.[10] In the past years, the potential prediction of theoretical $^1J_{CH}$ values for accurate structure elucidation and validation has been revisited by several authors.[11] We have compared our experimental results with those calculated by DFT,[11a] and a good correlation can be traced for all protons, although a general and systematic overestimation of the theoretical values by 2−3% exists (see Figure 3 and Table S1).

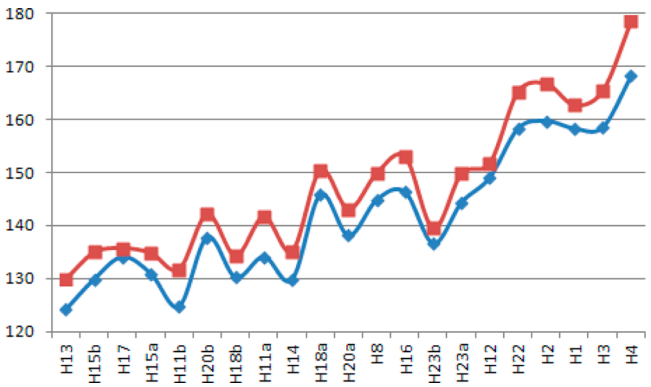

Figure 3. Correlation between experimental (blue; measured in this work) and theoretical (red; DFT calculations from ref 11a) $^1J_{CH}$ values (in Hz) in **1**. Note the systematic 2−3% overestimation of the theoretical values.

Figure 4 shows the $^1J_{CH}$ NMR profile of (+)-isopinocampheol (**2**) as an example of a molecule containing a strained bicyclo[3.1.1] skeleton. It is a good example demonstrating that $^1J_{CH}$ does not correlate with chemical shifts. As a quick view, all ^{1}H involved in the characteristic strained bridge shows $^1J_{CH}$ larger than usual [H1 (141.2 Hz), H5 (141.2 Hz), H7s (135.2 Hz), and H7a (136.8 Hz)], whereas all other aliphatic signals

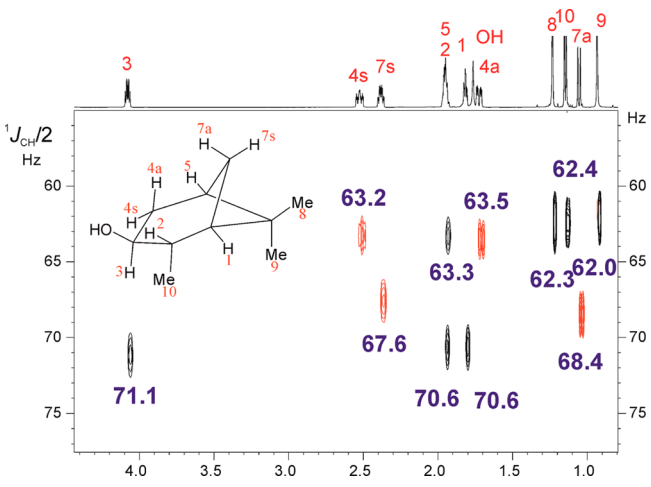

Figure 4. $^1J_{CH}$ NMR profile of (+)-isopinocampheol (**2**) in $CDCl_3$. The magnitude of $^1J_{CH}/2$ (in Hz) is extracted directly from the F_1 coordinate of each individual cross-peak.

present typical magnitudes in the range between 124 and 127 Hz. Also note the large $^1J_{CH}$ of H3 (142.2 Hz) due to the presence of the hydroxyl group and the efficient distinction between the fully overlapped H2 and H5 signals. Similarly, Figure 5 shows the $^1J_{CH}$ NMR profile of 2-exobromonorbor-

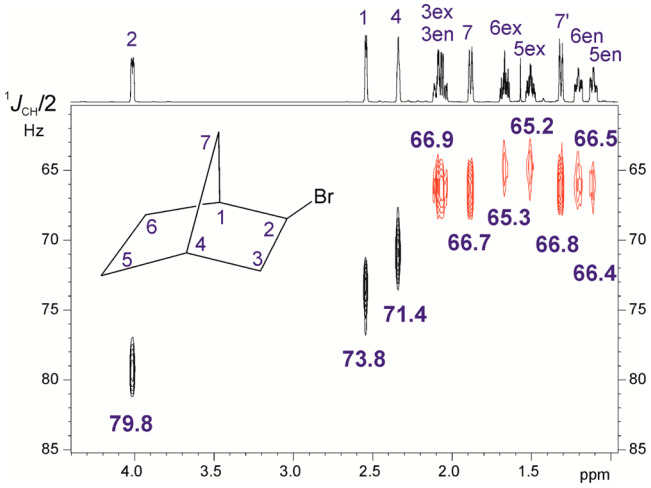

Figure 5. $^1J_{CH}$ NMR profile of 2-exobromonorbornane (**3**) in $CDCl_3$. The magnitude of $^1J_{CH}/2$ (in Hz) is extracted directly from the F_1 coordinate of each individual cross-peak.

nane (**3**), which contains a strained bicyclo[2.2.1] skeleton and an electronegative bromine substituent. At first sight, all CH_2 protons do not seem to show relevant $^1J_{CH}$ differences (between 130.4 and 133.6 Hz), but exo protons clearly present values (about 130.5 Hz) smaller than that of their endo pairs (about 133 Hz), demonstrating the excellent level of resolution achieved in F_1. On the other hand, the two bridged H1 and H4 protons have $^1J_{CH}$ values of 147.6 and 142.8 Hz, respectively, and the presence of Br is experimentally evidenced by the large $^1J_{CH}$ of H2 (159.6 Hz).

Even in the case where signal overlap precludes an accurate extraction of $^1J_{CH}$ due to the presence of similar $^1J_{CH}$ and $\delta(^1H)$, the analysis of the $^1J_{CH}$ profile can be used as a positive indicator for the absence of specific functionalities and differential structural elements. For instance, leaving aside its olefinic H4 proton (159.5 Hz), the steroid progesterone shows a characteristic fingerprinting with a large number of aliphatic ^{1}H resonances without a clear distinction of individual $^1J_{CH}$ (ranging from 124 to 130 Hz) (Figure S5). In a similar way, the $^1J_{CH}$ NMR profile of the carbohydrate sucrose shows a uniform and narrow range of $^1J_{CH}$ between 144.4 and 146.0 Hz, except for the H5 of the fructose ring (149.2 Hz) and the anomeric H1 proton (169.4 Hz) that confirms the α configuration in the glucose ring (Figure S6). These values completely agree with those reported previously.[5]

The HSQC-$^1J_{CH}$ can be recorded with a standard setup to monitor a wide range of $^1J_{CH}$ values. Because the key indirect dimension only displays doublets due to $^1J_{CH}$, these experiments can also be successfully recorded in the lowest magnetic fields, as shown for the antimalarial drug quinine at 400 MHz (Figure S7), where the accidental ^{1}H signal overlap in F_2 is the only potential drawback. Signal intensities in HSQC-$^1J_{CH}$ depend on several factors but mainly of the Δ delay optimization. Thus, a reoptimization of Δ can be required to observe very large $^1J_{CH}$ values, as found for the tryine derivative **4**,[12] which contains two terminal alkyne protons with $^1J_{CH}$

DOI: 10.1021/acs.joc.6b02873
J. Org. Chem. 2017, 82, 2040−2044

values around 251 Hz (Figure 6). In that particular case, a non-edited version of the HSQC-$^1J_{CH}$ pulse scheme (Figure S4)

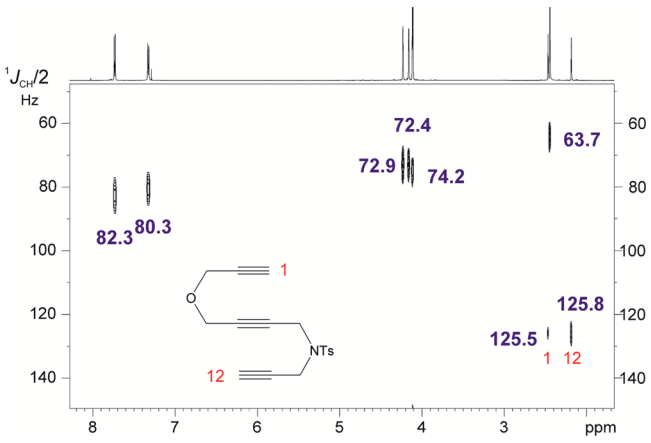

Figure 6. $^1J_{CH}$ NMR profile of the tryine derivative (**4**) in $CDCl_3$ obtained from a non-edited version of the pulse scheme of Figure 1 (optimized to 180 Hz). The magnitude of $^1J_{CH}/2$ (in Hz) is extracted directly from the *y* coordinate of each individual cross-peak.

optimized to 180 Hz has been used. In addition, broadband homodecoupling can be implemented in the F_2 dimension (Figure S8) to afford simplified *J* multiplet patterns, making it very easy to automate peak-picking (Figure S9).

CONCLUSIONS

In short, a new graphical interface to visualize and determine accurately the magnitude of $^1J_{CH}$ for all the protons of a molecule is now available. The advantage for using this intuitive $^1J_{CH}$ NMR profile is that the typical *J* measurement on doublets is avoided, minimizing common drawbacks associated with limited ^{1}H signal resolution and dispersion, multiplet complexity and distortions, or general applicability to any CH_n multiplicity, particularly when it comes to diastereotopic CH_2 protons. It has been shown that the simple determination of the F_1 coordinate in the $^1J_{CH}$ profile directly affords $^1J_{CH}/2$. In addition, this spectral representation provides a general and quick overview of all experimental $^1J_{CH}$, identifying key structural features, getting experimental evidence to the presence of representative functional groups, and facilitating stereochemical assignments. Without a doubt, further developments in complementary theoretical predictions of $^1J_{CH}$ will help in the use of these parameters in computer-assisted structure elucidation (CASE) and verification (ASV) programs.

EXPERIMENTAL SECTION

NMR experiments were recorded on a 600 MHz spectrometer equipped with a triple-resonance $^1H/^{13}C/^{15}N$ inverse probe. The temperature for all measurements was set to 298 K. All samples were prepared by dissolving 20 mg of the target molecule in the corresponding deuterated solvent. All products **1**, **2**, and **3** in the main text and **5**, **6**, and **7** in the Supporting Information were commercially available. The triene **4** was a loan from Prof. A. Roglans and Dr. A. Pla-Quintana from Universitat de Girona.

NMR spectra were recorded with proton 90° pulses of 8.5 μs and carbon 90° pulses of 10.5 μs. For broadband carbon inversion and refocusing, 0.5 ms smoothed chirp pulses (shape name: Crp60,0.5,20.1) and a four-chirp composite pulse of 2 ms duration (shape name: Crp60comp.4) were used, respectively, sweeping over a frequency band of 60 kHz. For the multiplicity editing block, the CRISIS (compensation of refocusing inefficiency with synchronized inversion sweep) approach was applied using two 1.73 ms refocusing pulses (shape name: Crp60_xfilt.2) as described in ref 7. Adiabatic ^{13}C decoupling (with 1.5 ms chirped pulses; shape name: Crp42,1.5,20.2) was applied during ^{1}H acquisition. The interpulse Δ delays in INEPT and BIRD elements were set to 3.57 ms ($\Delta = 1/(2*^1J_{CH})$; optimized to $^1J_{CH}$ = 140 Hz), and the recycle delay was set to 1 s. Two scans were accumulated for each one of the 256 t_1 increments, and the number of complex data points in t_2 was set to 2048. A basic two-step phase cycling is applied: $\phi_1 = x,-x$; $\phi_{rec} = x,-x$. Spectra were acquired with a spectral window of 6010 Hz (in F_2) and 250 Hz (in F_1), giving a FID resolution of 5.86 (F_2) and 1.95 (F_1) Hz, respectively. All experiments were acquired and processed using the echo/antiecho protocol where the gradient G1 was inverted for every second FID. Prior to Fourier transformation of the data, zero filling to 1024 in F_1 and a $\pi/2$-shifted squared cosine window function (QSINE, SSB: 2) in both dimensions were applied. Zero filling of the digital resolution was applied at 2.93 (F_2) and 0.24 (F_1) Hz, respectively. Gradient ratios for G1/G2 were set to 80:20.1 and measured as a percentage of the absolute gradient strength of 53.5 G/cm. Sine-bell-shaped gradients had 1 ms of duration and were followed by a recovery delay of 100 μs (δ). The final ZQF consists of a 30 ms chirped adiabatic pulse applied simultaneously to a rectangular gradient (G0 = 11%).

A java applet (jmeasurement.jar) for extracting $^1J_{CH}$ automatically from the HSQC-$^1J_{CH}$ spectrum is available on request. A script to automatically process the HSQC-$^1J_{CH}$ spectrum to afford the $^1J_{CH}$ NMR profile is available in the Mnova software package.

ASSOCIATED CONTENT

Supporting Information

The Supporting Information is available free of charge on the ACS Publications website at DOI: 10.1021/acs.joc.6b02873.

Experimental section, details of NMR spectra, and pulse program (PDF)

AUTHOR INFORMATION

Corresponding Author

*Tel: +34 935812291. E-mail: teodor.parella@uab.cat.

ORCID

Pau Nolis: 0000-0003-2360-1709

Teodor Parella: 0000-0002-1914-2709

Notes

The authors declare no competing financial interest.

ACKNOWLEDGMENTS

Financial support for this research provided by Spanish MINECO (Project CTQ2015-64436-P) is gratefully acknowledged. A.A.S. gratefully acknowledges support from the Brazilian agency CAPES (BEX 5382/15-7). We also thank to the Servei de Ressonància Magnètica Nuclear, Universitat Autònoma de Barcelona, for allocating instrument time to this project. NMR instrumentation at Carnegie Mellon University was partially supported by the NSF (CHE-0130903 and CHE-1039870). R.R.G. gratefully acknowledges support from the NSF (CHE-1111684).

REFERENCES

(1) (a) Hansen, P. E. *Prog. Nucl. Magn. Reson. Spectrosc.* **1981**, *14*, 175−295. (b) Contreras, R. H.; Peralta, J. E. *Prog. Nucl. Magn. Reson. Spectrosc.* **2000**, *37*, 321−345.

(2) (a) Enthart, A.; Freudenberger, J. C.; Furrer, J.; Kessler, H.; Luy, B. *J. Magn. Reson.* **2008**, *192*, 314−322. (b) Castañar, L.; Sistaré, E.; Virgili, A.; Williamson, R. T.; Parella, T. *Magn. Reson. Chem.* **2015**, *53*, 115−119. (c) Castañar, L.; Saurí, J.; Williamson, R. T.; Virgili, A.; Parella, T. *Angew. Chem., Int. Ed.* **2014**, *53*, 8379−8382.

DOI: 10.1021/acs.joc.6b02873
J. Org. Chem. 2017, 82, 2040−2044

(3) (a) Timári, I.; Kaltschnee, L.; Kolmer, A.; Adams, R. W.; Nilsson, M.; Thiele, C. M.; Morris, G. A.; Kövér, K. E. *J. Magn. Reson.* **2014**, *239*, 130−138. (b) Reinsperger, T.; Luy, B. *J. Magn. Reson.* **2014**, *239*, 110−120. (c) Kaltschnee, L.; Kolmer, A.; Timári, I.; Schmidts, V.; Adams, R. W.; Nilsson, M.; Kövér, K. E.; Morris, G. A.; Thiele, C. M. *Chem. Commun.* **2014**, *50*, 2512−2514. (d) Timári, I.; Kaltschnee, L.; Raics, M. H.; Roth, F.; Bell, N. G. A.; Adams, R. W.; Nilsson, M.; Uhrín, D.; Morris, G. A.; Thiele, C. M.; Kövér, K. E. *RSC Adv.* **2016**, *6*, 87848−87855.

(4) (a) Liu, M.; Farrant, R. D.; Gillam, J. M.; Nicholson, J. K.; Lindon, J. C. *J. Magn. Reson., Ser. B* **1995**, *109*, 275−283. (b) Fehér, K.; Berger, S.; Kövér, K. E. *J. Magn. Reson.* **2003**, *163*, 340−346. (c) Kövér, K. E.; Fehér, K. *J. Magn. Reson.* **2004**, *168*, 307−313. (d) Thiele, C. M.; Bermel, W. *J. Magn. Reson.* **2012**, *216*, 134−143. (e) Saurí, J.; Castañar, L.; Nolis, P.; Virgili, A.; Parella, T. *J. Magn. Reson.* **2014**, *242*, 33−40. (f) Snider, J. D.; Troche-Pesqueira, E.; Woodruff, S. R.; Gayathri, C.; Tsarevsky, N. V.; Gil, R. R. *Magn. Reson. Chem.* **2012**, *50*, S86−S91. (g) Castañar, L.; García, M.; Hellemann, E.; Nolis, P.; Gil, R. R.; Parella, T. *J. Org. Chem.* **2016**, *81*, 11126−11131. (h) Furrer, J.; John, M.; Kessler, H.; Luy, B. *J. Biomol. NMR* **2007**, *37*, 231−243.

(5) (a) Yu, B.; van Ingen, H.; Vivekanandan, S.; Rademacher, C.; Norris, S. E.; Freedberg, D. I. *J. Magn. Reson.* **2012**, *215*, 10−22. (b) Yu, B.; van Ingen, H.; Freedberg, D. I. *J. Magn. Reson.* **2013**, *228*, 159−165.

(6) Johnson, C. S., Jr *Prog. Nucl. Magn. Reson. Spectrosc.* **1999**, *34*, 203−256.

(7) Boyer, R. D.; Johnson, R.; Krishnamurthy, K. *J. Magn. Reson.* **2003**, *165*, 253−259.

(8) Thrippleton, M. J.; Keeler, J. *Angew. Chem., Int. Ed.* **2003**, *42*, 3938−3941.

(9) (a) Perlin, A. S.; Casu, B. *Tetrahedron Lett.* **1969**, *10*, 2921−2924. (b) Bock, K.; Wiebe, L. *Acta Chem. Scand.* **1973**, *27*, 2676−2678. (c) Juaristi, E.; Cuevas, G. *Acc. Chem. Res.* **2007**, *40*, 961−970.

(10) Thiele, C. M. *J. Org. Chem.* **2004**, *69*, 7403−7413.

(11) (a) Williamson, R. T.; Buevich, A. V.; Martin, G. E.; Parella, T. *J. Org. Chem.* **2014**, *79*, 3887−3894. (b) Kutateladze, A. G.; Mukhina, O. A. *J. Org. Chem.* **2015**, *80*, 10838−10848. (c) Venkata, C.; Forster, M. J.; Howe, P. W. A.; Steinbeck, C. *PLoS One* **2014**, *9*, e111576. (d) Helgaker, T.; Jaszunski, M.; Swider, P. *J. Org. Chem.* **2016**, *81*, 11496−11500.

(12) Fernández, M.; Ferré, M.; Pla-Quintana, A.; Parella, T.; Pleixats, R.; Roglans, A. *Eur. J. Org. Chem.* **2014**, *2014*, 6242−6251.

■ NOTE ADDED AFTER ASAP PUBLICATION

Reference 9c was added on January 24, 2017.

DOI: 10.1021/acs.joc.6b02873
J. Org. Chem. 2017, 82, 2040−2044